ARMY RESEARCH LABORATORY

Removing Full-scale Testing Barriers: Energetic Material Detonation Characterization at the Laboratory Scale

by Matthew M. Biss

ARL-TR-5943   **March 2012**

NOTICES

Disclaimers

The findings in this report are not to be construed as an official Department of the Army position unless so designated by other authorized documents.

Citation of manufacturer's or trade names does not constitute an official endorsement or approval of the use thereof.

Destroy this report when it is no longer needed.   Do not return it to the originator.

Army Research Laboratory

Aberdeen Proving Ground, MD 21005-5066

Removing Full-scale Testing Barriers:
Energetic Material Detonation Characterization
at the Laboratory Scale

Matthew M. Biss

Weapons and Materials Research Directorate, ARL

REPORT DOCUMENTATION PAGE

Public reporting burden for this collection of information is estimated to average 1 hour per response, including the time for reviewing instructions, searching existing data sources, gathering and maintaining the data needed, and completing and reviewing the collection information. Send comments regarding this burden estimate or any other aspect of this collection of information, including suggestions for reducing the burden, to Department of Defense, Washington Headquarters Services, Directorate for Information Operations and Reports (0704-0188), 1215 Jefferson Davis Highway, Suite 1204, Arlington, VA 22202-4302. Respondents should be aware that notwithstanding any other provision of law, no person shall be subject to any penalty for failing to comply with a collection of information if it does not display a currently valid OMB control number.
PLEASE DO NOT RETURN YOUR FORM TO THE ABOVE ADDRESS.

1. REPORT DATE (DD-MM-YYYY)	2. REPORT TYPE	3. DATES COVERED (From - To)
March 2012	Final	

4. TITLE AND SUBTITLE	5a. CONTRACT NUMBER
Removing Full-scale Testing Barriers: Energetic Material Detonation Characterization at the Laboratory Scale	5b. GRANT NUMBER
	5c. PROGRAM ELEMENT NUMBER
6. AUTHOR(S)	5d. PROJECT NUMBER
Matthew M. Biss	5e. TASK NUMBER
	5f. WORK UNIT NUMBER

7. PERFORMING ORGANIZATION NAME(S) AND ADDRESS(ES)	8. PERFORMING ORGANIZATION REPORT NUMBER
U.S. Army Research Laboratory ATTN: RDRL-WML-C Aberdeen Proving Ground, MD 21005-5066	ARL-TR-5943

9. SPONSORING/MONITORING AGENCY NAME(S) AND ADDRESS(ES)	10. SPONSOR/MONITOR'S ACRONYM(S)
	11. SPONSOR/MONITOR'S REPORT NUMBER(S)

12. DISTRIBUTION/AVAILABILITY STATEMENT

Approved for public release; distribution is unlimited.

13. SUPPLEMENTARY NOTES
Author email: <matthew.m.biss.civ@mail.mil>

14. ABSTRACT

A novel energetic-material detonation and air-blast characterization technique is proposed through the use of a laboratory-scale-based modified "aquarium test." A streak camera is used to record the radial shock wave expansion rate at the energetic material–air interface of spherical laboratory-scale (*i.e.*, gram-range) charges detonated in air. A linear regression fit is applied to the measured streak record data. Using this in conjunction with the conservation laws, material Hugoniots, and two empirically established relationships, a procedure is developed to determine fundamental detonation properties (pressure, velocity, particle velocity, and density) and air shock wave properties (pressure, velocity, and particle velocity) at the energetic material–air interface. The experimentally determined properties are in good agreement with published values. The theory's applicability is extended using historical aquarium test data due to the limited number of experiments able to be performed. Predicted detonation wave and air shock wave properties are in good agreement for a multitude of energetics across various atmospheric conditions.

15. SUBJECT TERMS

Aquarium test, Detonation characterization, Air-blast characterization, Shock wave, Laboratory-scale, Spherical charges

16. SECURITY CLASSIFICATION OF:			17. LIMITATION OF ABSTRACT	18. NUMBER OF PAGES	19a. NAME OF RESPONSIBLE PERSON
a. REPORT	b. ABSTRACT	c. THIS PAGE	UU	34	Matthew M. Biss
Unclassified	Unclassified	Unclassified			19b. TELEPHONE NUMBER (Include area code) 410-278-3708

Contents

List of Figures

List of Tables

Acknowledgments

1. Introduction

The experimental determination of an energetic material's damage potential is characterized by the detonation wave and air shock wave properties produced as a result of its rapid decomposition. The key detonation wave properties needed for characterization include: detonation or Chapman-Jouguet (CJ) pressure P_{CJ}, detonation wave velocity D, reaction products particle velocity u_{CJ}, and reaction products density ρ_{CJ}. The ultra-high-speed nature of the detonation event involves nanosecond timescale chemical reactions, producing temperatures between 2000–5000 K, pressures upwards of 50 GPa, and detonation wave velocities ranging from 4–10 mm/μs (*1–3*). Experimentally measuring these properties presents a difficult challenge due to the severe nature of the environment and the temporal scale on which they occur. Presently, to determine the desired detonation wave properties, a multitude of experiments (many conducted using kg-range charges) and instrumentation are necessary. These can include piezoelectric-pin instrumented detonation velocity experiments, plate dent or aquarium test experiments, and photon Doppler velocimetry experiments, to name a few. Thus, the current detonation characterization protocol ultimately limits the development of novel energetic formulations as it tends to become cost prohibitive.

Early detonation characterization research on the detonation wave reaction-zone length and pressure was first suggested by Goranson in 1946 (*4*). He determined that the reaction-zone length and CJ pressure for an energetic material could be determined through free-surface velocity measurements of metal "flyer plates" positioned adjacent to an energetic charge. Duff and Houston later tested this theory by characterizing Composition B using aluminum flyer plates of various thicknesses (*5*). Further detonation characterization was conducted by Holton, who extrapolated CJ pressures using the "aquarium test," an extension to Goranson's flyer-plate experiment, in which the flyer plate is replaced by an optically transparent material (most commonly, water) (*6*). In this test, a streak image is taken parallel to the axis of a sympathetically detonated cylindrical explosive charge submerged in a container filled with distilled water. The recorded streak record is subsequently analyzed to determine the time-dependent position of the outward-propagating shock wave. An empirical shock wave distance-versus-time relationship is applied to the data and from this, the shock wave velocity at the water–charge interface may be determined through its differentiation and extrapolation to the water–charge interface. From this, a detonation pressure is calculated using Goranson's equation with the known Hugoniot for water and known energetic material and water densities (*7*).

Further aquarium test research was conducted by Rigdon and Akst to determine the optimum procedure for extrapolating the shock wave velocity at the material interface, as aquarium test detonation pressures were consistently lower than published values (*8*). A host of empirical curvefitting techniques were applied to a range of data sets to determine the optimum treatment of the shock wave radius-versus-time data. They concluded that a linear regression fit to the initial 2 mm of shock wave travel (7.2 cm charge diameter) yielded the highest-accuracy results when compared to published values.

Conducting the air shock wave characterization of energetic materials presents a similarly challenging environment due to the pressures and temperatures being transferred into the surrounding medium. Air shock wave characterization properties of interest include the shock wave pressure P, shock wave velocity U, particle velocity u, explosive impulse I, and more recently of interest, fireball temperatures T (*9*). Air shock wave characterization is traditionally conducted using kg-range charges instrumented with piezoelectric or piezoresistive pressure transducers positioned at specified radial standoff distances. These transducers measure the shock wave time of arrival, peak shock wave pressure, and explosive impulse, and allow a shock wave velocity to be determined given multiple transducers. Due to the harsh nature of the environment, however, measurements are rarely taken at radial standoffs of <5 charge diameters, providing little data suitable towards deriving the detonation wave or air shock wave properties at the energetic material–air interface.

In response to these aforementioned shortcomings, a laboratory-scale-based modification of the aquarium test has been developed to allow both the detonation wave and the air shock wave properties at the energetic material–air interface to be determined from a single experimental measurement. The optically based method incorporates high-speed photography and laboratory-scale (*i.e.*, gram-range) spherical explosive charges. The detonation wave and air shock wave properties for an energetic material of interest may be determined from material Hugoniots, conservation laws, two empirically established relationships, and a single film-based streak record. The laboratory-scale-based method provides an accurate, cost-effective, characterization procedure for novel energetic materials as an alternative to the full-scale characterization experiments currently used.

2. Theory/Methodology

A shock wave is fully defined through knowledge of five state variables: shock pressure P, shock velocity U, particle velocity u, density ρ or specific volume v, and specific internal energy e. These variables are defined by the conservation of mass (equation 1), momentum (equation 2), and energy (equation 3) jump equations across the shock wave (subscripts 0 and 1 refer to the states before and after the shock's passage). In order to solve for the shock wave's state, two additional relationships are necessary. The first relationship is an equation of state for the material of interest. The desired equation of state would relate the specific internal energy as a function of pressure and specific volume, *i.e.*, $e = f(P, v)$. By combining it with the conservation of energy jump equation (equation 3), the specific internal energy is eliminated, leaving the well-known Hugoniot equation, equation 4. The Hugoniot equation describes the loci of pressure states attainable after a shock wave's passage through a material as a function of the material's specific volume. This reduces to four variables (P, U, u, and v) in three equations (equations 1, 2, and 4). Thus, if an additional relationship may be determined between the four remaining variables, the system is closed.

$$\frac{\rho_1}{\rho_0} = \frac{U - u_0}{U - u_1} = \frac{v_0}{v_1} \tag{1}$$

$$P_1 - P_0 = \rho_0(u_1 - u_0)(U - u_0) \tag{2}$$

$$e_1 - e_0 = \frac{P_1 u_1 - P_0 u_0}{\rho_0(U - u_0)} - \frac{1}{2}(u_1^2 - u_0^2) \tag{3}$$

$$P = f(v) \tag{4}$$

Material Hugoniots are experimentally measured by subjecting a material to a series of known shock compression experiments. A total of six Hugoniot "planes," or pairs, may be determined based on the four remaining state variables: $P - U$, $P - u$, $P - v$, $U - u$, $U - v$, and $u - v$. Of these, three planes have been found to be of great importance when analyzing shock wave interactions: $U - u$, $P - v$, and $P - u$. Thus, adding the $U - u$ or $P - u$ Hugoniot relationship allows the shock wave's state to be fully defined. By extending these equations to the interaction

3

of an energetic material detonating in a surrounding fluid medium, each material's "shocked" state may therefore be determined.

Using these equations, it is proposed to calculate the detonation wave and transmitted shock wave properties at the interface of an energetic material detonating in air through the sole measurement of the air shock wave velocity U. From this measurement, the following seven properties are to be solved: detonation wave velocity D, detonation wave pressure P_{CJ}, reaction products particle velocity u_{CJ}, reaction products density ρ_{CJ}, air shock wave pressure P, air particle velocity u, and air density ρ. Thus, a system of seven equations is necessary to define the detonation interaction.

The first two equations implemented are the conservation of mass and momentum equations across a detonation wave. Here, the equations are written for the case of a one-dimensional planar detonation wave. Conservation of mass (equation 1) is rewritten for the detonating energetic material, yielding equation 5. For this, the density ratio is the reaction products density ρ_{CJ} divided by the energetic material pressing density ρ_e, detonation velocity D is substituted for the shock wave velocity U, and the reaction products particle velocity u_{CJ} replaces the particle velocity behind the detonation wave u_1. The particle velocity ahead of the detonation wave u_0 is zero as the material is yet to be affected by the detonation.

$$\frac{\rho_{CJ}}{\rho_e} = \frac{D}{D - u_{CJ}} \tag{5}$$

Detonation wave property variables are additionally substituted into the conservation of momentum equation (equation 2). The previous conservation of mass substitutions remain valid and the pressure ahead of the detonation wave is assumed to be zero as $P_0 \ll P_{CJ}$. Thus, conservation of momentum across the detonation wave is represented by

$$P_{CJ} = \rho_e u_{CJ} D \quad . \tag{6}$$

When the outward propagating detonation wave reaches the energetic material–air interface, a transmitted shock wave is produced and driven radially outward through the air by the expanding energetic material reaction products (*10*). As a result of this interaction, a rarefaction wave is driven rearward through the reaction products toward the point of initiation (*2*). To satisfy the laws of conservation, the pressure and particle velocity at the energetic material–air interface must be equal for the forward propagating transmitted shock wave and the rearward propagating

4

rarefaction. Thus, if a pressure–particle velocity ($P - u$) Hugoniot is known for both the energetic material reaction products and air, a solution for the pressure and particle velocity at the interface is determinable.

Presently, there exists a limited collection of Hugoniot data for energetic material reaction products due to the numerous existing explosives and their multiple densities incorporated throughout the field. In response to this, Cooper developed a non-dimensional empirical relationship from published $P - u$ Hugoniot data for energetic material reaction products (*2*). He discovered that if the compilation of existing Hugoniot data are plotted in a reduced form, *i.e.*, reduced pressure P/P_{CJ} and reduced particle velocity u/u_{CJ}, they collapse to a single profile, represented by two empirical relationships (*2*). This profile is divided into two equations based upon the reduced pressure value. For reduced pressures greater than 0.08, the reduced reaction products Hugoniot is represented by equation 7 and has a coefficient of determination of 0.987.

$$\frac{P}{P_{CJ}} = 2.412 - 1.7315\left(\frac{u}{u_{CJ}}\right) + 0.3195\left(\frac{u}{u_{CJ}}\right)^2 \tag{7}$$

For reduced pressures less than 0.08, the reduced reaction products Hugoniot is represented by equation 8 and has a coefficient of determination of 0.898.

$$\frac{P}{P_{CJ}} = 235\left(\frac{u}{u_{CJ}}\right)^{-8.71} \tag{8}$$

For the present case, the reduced pressure is anticipated to be extremely low due to the large shock impedance discrepancy between the energetic material and air. Shock impedance Z is defined as the product of a material's density and shock wave velocity (*2*), equation 9. The energetic material impedance Z_e is defined as the product of its pressing density ρ_e and its detonation velocity D (equation 10), whereas air's shock impedance Z_{air} is defined as the product of its ambient density ρ_{air} and the transmitted shock wave velocity U (equation 11). The energetic material pressing density is ~1500 times greater than the density of air. If it is assumed that the detonation wave velocity and air shock wave velocity are of approximately the same order of magnitude, the detonation wave interaction with air results in a transmitted shock wave having a pressure less than the detonation pressure P_{CJ} and a particle velocity greater than u_{CJ} according to the material Hugoniots (figure 1). Knowledge of the air shock wave–particle velocities relationship is required to determine how low this reduced pressure will be. It should be noted that each material's impedance is not constant and that both will increase slightly with

increasing pressure. However, for practical purposes, the shock impedances may be considered constant across a reasonable range of interest (*2*).

$$Z = \rho U \tag{9}$$

$$Z_e = \rho_e D \tag{10}$$

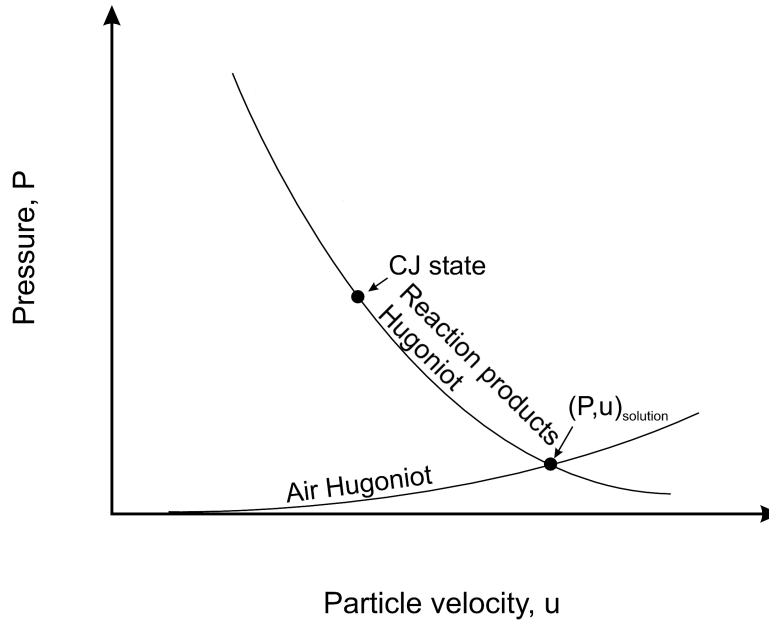$$Z_{air} = \rho_{air} U \tag{11}$$

Figure 1. Interface interaction on the $P - u$ Hugoniot plane.

Previous research has shown that, for most materials, a linear relationship exists between the shock wave and particle velocities, or the $U - u$ Hugoniot (figure 2). The linear relationship is composed of two empirically measured coefficients: C_0, defined as the bulk sound speed (though it has no physical meaning) and s, corresponding to the $U - u$ Hugoniot slope, equation 12. The $U - u$ Hugoniot coefficients for air are well established from previous research by Deal who conducted plate impact experiments using explosively driven flyer plates. In his research, he determined air's Hugoniot coefficient C_0 to be 0.2375 km/s and s to be 1.0575 for measured shock wave velocities up to 4.5 km/s. A higher shock wave velocity is expected, however, air's

Hugoniot is assumed to remain linear throughout the measurement regime. Given that the air shock wave velocity is linearly related to the particle velocity (equation 12) and the energetic material pressing density is ~1500 times greater than the density of air, an extremely large impedance mismatch between the materials results, and ultimately, a much lower pressure is produced (*2*). Thus, the reduced pressure may be anticipated to fall below the 0.08 established threshold, and equation 8 is used for solving the system. Lastly, it should be noted that the $U - u$ Hugoniot for air is used in place of the $P - \rho$ Hugoniot as it has previously been well characterized.
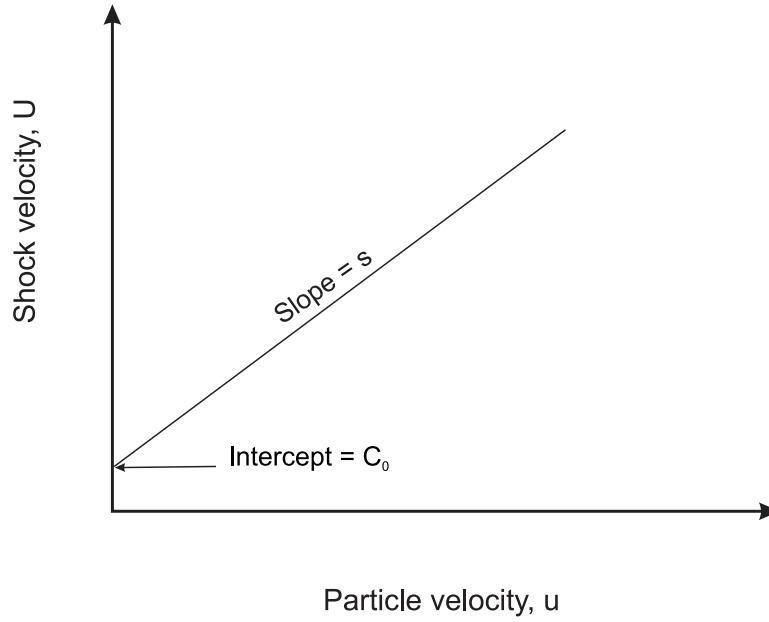

Figure 2. $U - u$ Hugoniot plane.

$$U = C_0 + su \tag{12}$$

As shown by figure 1, an equation representing the $P - u$ Hugoniot plane for air is required to determine the shock wave pressure and particle velocity solution to the energetic material–air interaction. This is obtained by combining the conservation of momentum equation (equation 2) and air's $U - u$ Hugoniot relation, yielding equation 13. As with conservation of momentum across the energetic material detonation wave (equation 6), the shock wave velocity, shock wave pressure, and particle velocity ahead of the shock wave (U_0, P_0, and u_0 in equation 2, respectively) are zero, as the air is yet to be affected by the detonation and $P_0 \ll P$. Thus, given equations 8 and 13, a solution for the shock wave pressure and particle velocity at the energetic material–air interface is determinable by plotting the two $P - u$ Hugoniots.

7

$$P = \rho_{air} C_0 u + \rho_{air} s u^2 \tag{13}$$

The final equation required to define the air shock wave is the conservation of mass written for across a shock wave, equation 14. For this, the density ratio is the air shock wave density ρ divided by the atmospheric density ρ_{air}, the shock wave particle velocity u is the particle velocity behind the detonation wave u_1, and the shock wave velocity U remains. As before, the shock wave velocity, shock wave pressure, and particle velocity ahead of the shock wave (U_0, P_0, and u_0, respectively) are zero, as the air is yet to be affected by the detonation and $P_0 \ll P$.

$$\frac{\rho}{\rho_{air}} = \frac{U}{U - u} \tag{14}$$

The final equation required to close the system is an empirical relationship developed by Cooper (2) that relates the reaction products density to the energetic material pressing density, equation 15. This is chosen in place of a $P - \rho$ Hugoniot for the reaction products as no all-energetic-material-encompassing Hugoniot exists. Equation 15 is shown to be valid for densities ranging between $2e^{-3}$– 9 g/cm^3.

$$\rho_{CJ} = 1.386 \rho_e^{0.96} \tag{15}$$

By solving the system of equations, the desired detonation wave properties (D, P_{CJ}, u_{CJ}, and ρ_{CJ}) and air shock wave properties at the interface (P, u, and ρ) are determinable for an energetic material of interest by measuring the air shock wave velocity U at the energetic material–air interface. The system solution is represented by equations 16–22:

$$u = \frac{U - C_0}{s} \tag{16}$$

$$P = \rho_{air} C_0 u + \rho_{air} s u^2 \tag{17}$$

$$\rho_{CJ} = 1.386 \rho_e^{0.96} \tag{18}$$

$$u_{CJ} = exp \; \dfrac{\ln \left(\dfrac{Pu^{8.71}}{235 \dfrac{\rho_{CJ}\rho_e}{\rho_{CJ} - \rho_e}} \right)}{10.71} \tag{19}$$

$$D = \dfrac{u_{CJ}\rho_{CJ}}{\rho_{CJ} - \rho_e} \tag{20}$$

$$P_{CJ} = \rho_e u_{CJ} D \quad . \tag{21}$$

$$\rho = \dfrac{U\rho_{air}}{U - u} \tag{22}$$

3. Experimental Methods

3.1 Spherical Charges

Centrally initiated laboratory-scale spherical charges are used to eliminate the critical diameter effect associated with energetic-material detonations (*11*). As previously mentioned, the conservation equations developed are written for the case of a planar shock wave interaction. However, previous research has demonstrated that the radial divergence effects associated with spherical detonation waves are insignificant for shock wave curvatures that are orders-of-magnitude larger than the detonation-reaction-zone thickness (*12–15*). Thus, the planar equations remain valid for the present explosive charge configuration.

Spherical charges are composed of matching hemispheres having a nominal equivalent mass of 0.90 g. Each hemisphere possesses a centrally positioned half right-circular-cylinder void to accommodate a RP-3 exploding bridgewire (EBW) detonator (29 mg pentaerythritol tetranitrate [PETN]), when assembled as shown in figure 3. Charges are composed of Class V RDX pressed to a density of 1.77 or 1.63 g/cm^3. The assembled charge masses m and their respective densities ρ_e are tabulated in table 1.
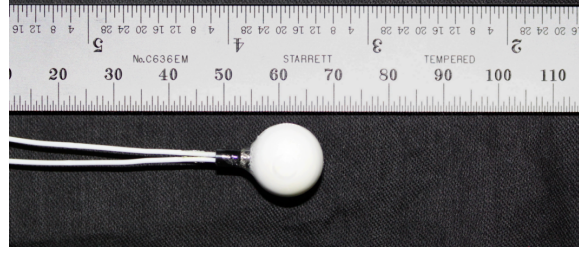
Figure 3. Fully assembled spherical charge with RP-3 EBW detonator.

Table 1. Experimental charges detonated.

Charge	ρ_e (g/cm^3)	m (g)
11318-3	1.77	1.809
11318-4	1.77	1.814
12040-2	1.63	1.779
12040-4	1.63	1.749
12052-1	1.63	1.726
12052-3	1.63	1.758

3.2 Charge Imaging

A Beckman & Whitley, Model 770 synchronized film-based streak camera is used to record the explosively driven air shock wave radial expansion. The streak camera has a slit width of 0.1 mm and a write speed of 8 mm/μs. A 90 cm $f/6.3$ field lens is used to relay a focused image onto the streak camera film plane. Figure 4 shows the experimental setup used for the present experiments. The explosive fireball and ionization of the surrounding air due to the shock wave provide self-illumination of the record from which radial expansion rates are measurable. A geometric correction factor is not implemented into the present measurements as the angles associated with the radial expansion measurements are extremely small (*i.e.*, $\mathcal{O}$(mrads)) , therefore allowing the small-angle approximation.
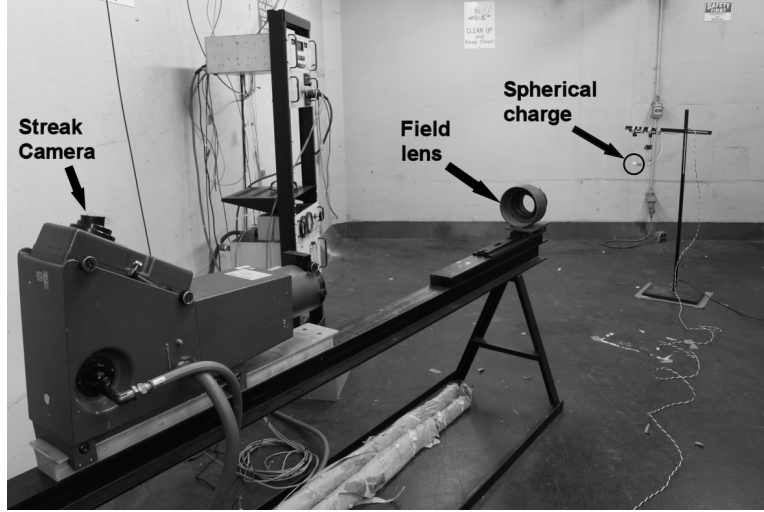
10

Figure 4. Experimental imaging setup.

4.   Results and Discussion

4.1   Experimental Results

Prior to conducting an experiment, a static image of a calibration object (here, a dimensional scale) was recorded to determine image magnification, and ultimately, a calibration length scale. Spherical charges were oriented with the cylindrical detonator axis collinear to the slit to ensure the transferred air shock wave measured was produced by a steady-state detonation and normal to the slit axis (figure 5). As shown, two fiducial wires were oriented perpendicular to the slit axis at the streak camera image plane to allow charge orientation and position to be determined between static and streak images. The explosive fireball illumination and air shock wave ionization were used for film exposure. This produced an acceptable streak record (50 μs total), as only the initial 130 ns were necessary for the present research (figure 6).

Streak records were analyzed on a vertical-beam optical comparator (S-T Industries, Inc. Model 4600) with 20X objective lens. Measurements were taken at 0.05-mm intervals along the temporal axis, corresponding to a radial shock wave measurement taken every 6.25 ns. Data were subsequently transformed into dimensional shock wave radius and time coordinates using the calibration length scale and known write speed. A best-fit linear correlation was determined for each data set according to equation 23, which consists of the shock wave radius R, air shock
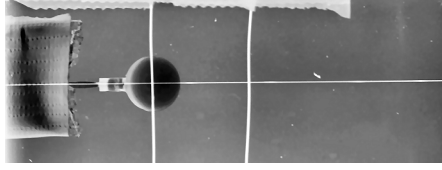
Figure 5. Static image of charge–slit orientation.

Figure 6. Sample streak record at 8 mm/μs writing speed (time=ordinate and radius=abscissa) .

wave velocity U, time t, and the spherical charge radius r_0. Only the initial 1.2 mm of radial shock wave travel were measured according to the results of Rigdon and Akst (*8*). From their research, it was determined that a linear correlation fit to the initial 2 mm of radial shock wave travel yielded the highest accuracy for determining detonation pressures from aquarium experiments. However, their research incorporated energetic charges having diameters of 7.2 cm. Using the explosive scaling laws, it was determined that only the first 1.2 mm of radial shock wave travel were necessary for accurate reduction of the current data. Resulting data and the average linear regression fit are shown in figures 7 and 8.
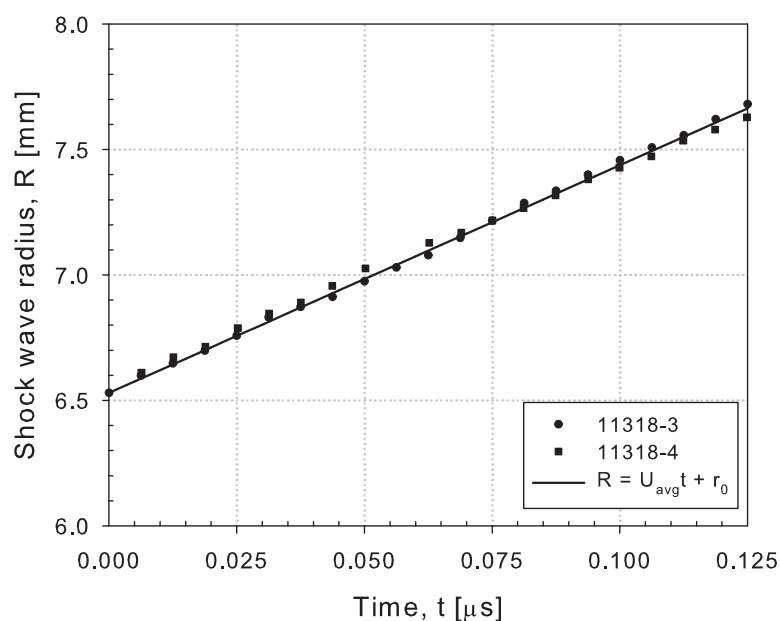
$$R = Ut + r_0 \tag{23}$$

Figure 7. Shock wave radius-versus-time data for RDX at 1.77 g/cm^3 with average linear regression fit.
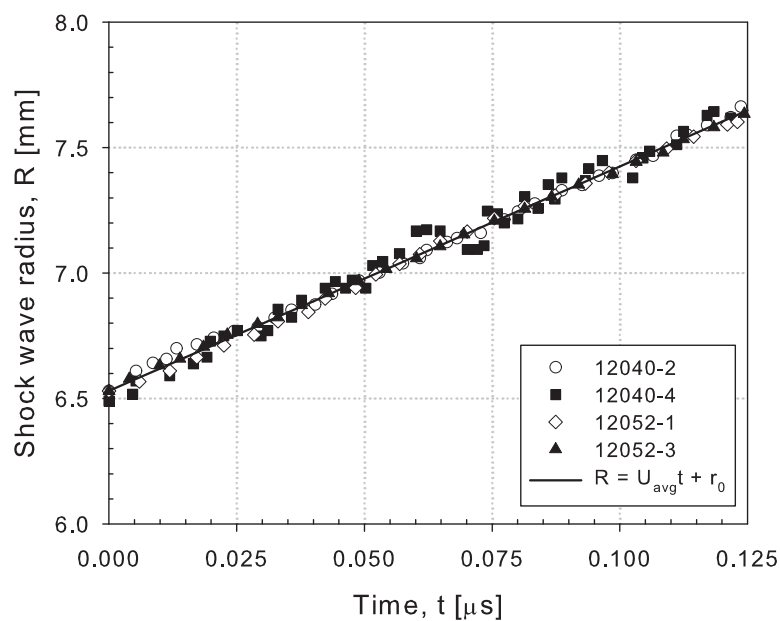

Figure 8. Shock wave radius-versus-time data for RDX at 1.63 g/cm^3 with average linear regression fit.

The shock wave velocity was determined from the best-fit linear correlation to the data and input into a MATLAB script written to calculate the desired characterization properties. The script allows the user to input the energetic material pressing density ρ_e and the ambient density of air ρ_{air} at the time of experiment. Detonation wave and air shock wave properties were subsequently solved for each experiment according to equations 16–22. Experimental results are tabulated in tables 2 and 3.

Table 2. Calculated detonation wave and air shock wave properties for RDX at 1.77 g/cm^3.

Explosive	$\rho_{\mathbf{air}}$ (g/cm^3)	U (mm/μs)	D (mm/μs)	$P_{\mathbf{CJ}}$ (GPa)	$\rho_{\mathbf{CJ}}$ (g/cm^3)	$u_{\mathbf{CJ}}$ (mm/μs)	P (MPa)	ρ (g/cm^3)	u (mm/μs)
Published	-	-	8.69 (*16*)	33.6 (*17*)	2.34 (*2*)	-	-	-	-
11318-3	$1.202e^{-3}$	9.18	8.73	35.3	2.40	2.28	93.3	$1.532e^{-2}$	8.46
11318-4	$1.202e^{-3}$	8.96	8.51	33.6	2.40	2.23	88.9	$1.517e^{-2}$	8.25
Average	$1.202e^{-3}$	9.07	8.62	34.4	2.40	2.26	91.1	$1.524e^{-2}$	8.36
% Deviation	-	-	0.81	2.53	2.56	-	-	-	-

Table 3. Calculated detonation wave and air shock wave properties for RDX at 1.63 g/cm^3.

Explosive	$\rho_{\mathbf{air}}$ (g/cm^3)	U (mm/μs)	D (mm/μs)	$P_{\mathbf{CJ}}$ (GPa)	$\rho_{\mathbf{CJ}}$ (g/cm^3)	$u_{\mathbf{CJ}}$ (mm/μs)	P (MPa)	ρ (g/cm^3)	u (mm/μs)
Published	-	-	8.34 (*16*)	28.3 (*17*)	2.16 (*2*)	-	-	-	-
12040-2	$1.207e^{-3}$	8.85	8.40	30.4	2.22	2.22	87.0	$1.504e^{-2}$	8.14
12040-4	$1.207e^{-3}$	9.06	8.61	31.9	2.22	2.28	91.2	$1.519e^{-2}$	8.34
12052-1	$1.213e^{-3}$	9.16	8.71	32.7	2.22	2.31	93.7	$1.543e^{-2}$	8.44
12052-3	$1.206e^{-3}$	8.74	8.30	29.7	2.22	2.19	84.8	$1.506e^{-2}$	8.04
Average	$1.208e^{-3}$	8.95	8.51	31.2	2.22	2.25	89.2	$1.518e^{-2}$	8.24
St. Dev.	$3.202e^{-6}$	0.19	0.19	1.4	0.00	0.05	4.0	$1.794e^{-4}$	0.18
% Deviation	-	-	1.98	10.2	2.78	-	-	-	-

The percent deviation between average and published values was determined using equation 24. As shown by tables 2 and 3, the detonation wave properties (D, P_{CJ}, and ρ_{CJ}) were all within 3% of their published values with the exception of the detonation pressure for the 1.63 g/cm^3 charges, which was found to be 10.2%. It should be noted, however, that the published detonation pressure for RDX pressed to 1.63 g/cm^3 was empirically derived by Keshavarz as an experimentally measured value was unavailable (*17*). Thus, the presently calculated deviation would be affected by the inherent empirical error associated with the published value.

$$\text{\% deviation} = \frac{|\text{average - published}|}{\text{published}} * 100 \tag{24}$$

An analysis was performed to determine the inherent uncertainty within the calculated data due to the experimental uncertainty present and empirical relationships employed according to Moffat (*18*). The uncertainty in measuring the air shock wave velocity U was calculated from the experimental uncertainties introduced as a result of measuring the initial charge radius ($\Delta r_0 = 0.005$ mm), shock wave radius ($\Delta R = 0.005$ mm), and time ($\Delta t = 6.25e^{-5}\mu$s). This led to an uncertainty of 0.09 mm/μs for the air shock wave velocity U and 0.08 mm/μs for the air particle velocity u. The uncertainty in the calculated reaction products density ρ_{CJ} was determined to be $6.5e^{-3}$ g/cm^3, resulting from the experimental uncertainty in the pressing density measurement. These uncertainties, in addition to the uncertainties in the atmospheric density at the time of test, produced an uncertainty of 2 MPa for the calculated air shock wave pressure P. The reaction products particle velocity u_{CJ} possessed an uncertainty of 0.02 mm/μs and the detonation wave velocity D had an uncertainty of 0.14 mm/μs. Lastly, the detonation pressure P_{CJ} uncertainty was determined to be 0.025 GPa. Thus, for all properties calculated, the experimental uncertainty was determined to be less than 2% of their respective values.

4.2   Historical Data

The proposed theory was applied to previous research incorporating variants of the aquarium test to determine the detonation wave and air shock wave properties of an energetic material. The research allowed the present method to be applied to a range of full-scale (*i.e.*, kg-range) energetic charges across various atmospheric conditions (*10, 19, 20*). The tests consisted of experimentally measuring multiple variables for a given explosive as well as having *a priori* knowledge of the energetic material's reaction products Hugoniot or detonation variables. In each case, the measured air shock wave velocity at the interface and atmospheric density were input into the MATLAB script, allowing all other detonation wave and air shock wave properties to be calculated. The results for several cases are reported in table 4. Air shock wave density at the interface was not reported in any references and was therefore disregarded in the present results. The developed theory was able to predict the published values within 6% (equation 25) for all properties, while the majority were predicted within 3%, as shown by the tabulated results. Thus, the theory's accuracy was extended using historical characterization research. This also demonstrates the theory's utility as the only properties required to perform a fundamental detonation characterization on an energetic material of interest are the pressing density, atmospheric density, and the initial shock wave velocity.

15

$$\% \text{ deviation} = \frac{|calculated \text{ - } published|}{published} * 100 \qquad (25)$$

Table 4. Calculated detonation wave and air shock wave properties from previous experimental research.

Explosive	ρ_e (g/cm^3)	ρ_air (g/cm^3)	U (mm/μs)	D (mm/μs)	P_CJ (GPa)	ρ_CJ (g/cm^3)	P (MPa)	u (mm/μs)
HMX/Inert (19) (95/5)	1.781	$1.068e^{-2}$	7.42	8.73	33.5	2.34	53.0	6.53
Calculated	-	-	-	8.60	34.5	2.41	53.8	6.79
% Deviation	-	-	-	1.5	3.0	2.9	1.5	4.0
HMX/TNT/Inert (19) (68/30/2)	1.776	$3.785e^{-3}$	7.84	8.21	31.2	2.40	21.2	7.13
Calculated	-	-	-	8.26	31.7	2.41	21.3	7.18
% Deviation	-	-	-	0.6	1.7	0.4	0.5	0.7
TNT (10)	1.636	$0.971e^{-3}$	7.34	6.93	20.7	2.15	47.8	6.71
Calculated	-	-	-	6.80	20.0	2.22	47.8	6.71
% Deviation	-	-	-	1.9	3.4	3.2	0	0
Composition B (10) (Grade A)	1.717	$0.947e^{-3}$	8.67	7.98	29.5	2.34	65.5	7.97
Calculated	-	-	-	8.05	29.2	2.33	65.5	7.98
% Deviation	-	-	-	0.9	1.0	0.4	0	0.1
Cyclotol (10) (77/23)	1.752	$0.936e^{-3}$	8.64	8.27	31.3	2.38	64.2	7.94
Calculated	-	-	-	8.01	29.5	2.37	64.2	7.95
% Deviation	-	-	-	3.1	5.8	0.4	0	0.1
Octol (10) (77.6/22.4)	1.821	$0.943e^{-3}$	8.86	8.49	34.2	2.46	68.1	8.14
Calculated	-	-	-	8.23	32.2	2.46	68.1	8.15
% Deviation	-	-	-	3.1	5.8	0	0	0.1
HBX-1 (20)	1.712	$1.253e^{-3}$	7.61	7.31	22.0	2.18	67.0	6.97
Calculated	-	-	-	7.22	22.4	2.21	66.5	6.97
% Deviation	-	-	-	1.2	1.8	1.4	0.7	0

5.   Conclusion

A laboratory-scale-based modification of the aquarium test has been provided for the detonation wave and air shock wave characterization of energetic materials. The technique measures the radial shock wave expansion rate produced at the energetic material–air interface from the detonation of laboratory-scale spherical charges. Air shock wave velocities were measured by fitting a regression line to the first 1.2 mm of streak record data. From this measurement, a procedure was developed to determine fundamental detonation wave and air shock wave properties for an energetic material of interest through use of conservation laws, material Hugoniots, and two empirically established relationships. The theory was verified using pressed RDX spheres and historical aquarium test data.

The developed theory allows a fundamental characterization to be performed from a single laboratory-scale experiment requiring minimal energetic material, offering a highly advantageous, cost-saving approach for the screening of novel energetic formulations. Thus, it provides an alternative to the multitude of full-scale experimental characterization techniques currently employed during the developmental phase of novel energetic formulations. Presently, to determine the desired detonation wave (velocity D, pressure P_{CJ}, particle velocity u_{CJ}, and density ρ_{CJ}) and air shock wave (pressure P and particle velocity u) properties, a multitude of experiments (many conducted using kg-range charges) and instrumentation are necessary. However, as shown by the experimental and historical data, the present theory only requires a single experimental measurement to obtain all of the above-named properties. The theory's utility is apparent as it provides fundamental energetic material detonation wave and air shock wave (at the energetic material–air interface) characterization properties from only a few grams of material. Additional testing is necessary, however, to validate the theory for a wider range of energetic formulations. Energetics exhibiting large reaction-zone thickness, critical diameter, and energy fluence should be tested to verify the technique's validity. Lastly, it is recommended that numerical modeling be performed to ensure that the assumed second-order spherical divergence effects are indeed negligible for the proposed laboratory-scale charges.

6. References

1. Tarver, C. Detonation reaction zones in condensed explosives. In *AIP Conference Proceedings*; Vol. 845; 2006.

2. Cooper, P. *Explosives engineering*; Wiley-VCH, Inc: New York, 1996.

3. Keshavarz, M.; Nazari, H. A simple method to assess detonation temperature without using any experimental data and computer code. *Journal of Hazardous Materials* **2006**, *133* (1–3), 129–134.

4. Goranson, R. W. *A method for determining E.O.S and reaction zones of high explosives and its application to Pentolite, Composition B, Buretol, and TNT*; LA-487; Los Alamos Scientific Laboratory: Los Alamos, NM, 1946.

5. Duff, R.; Houston, E. Measurement of the Chapman-Jouguet pressure and reaction zone length in a detonating high explosive. *The Journal of Chemical Physics* **1955**, *23* (7), 1268.

6. Holton, W. *The detonation pressures in explosives as measured by transmitted shocks in water*; NAVORD Report 3968; Naval Ordnance Laboratory: White Oak, MD, December 1954.

7. Suceska, M. *Test methods for explosives*; Springer-Verlag: New York, 1995.

8. Rigdon, J. K.; Akst, I. B. An analysis of the "Aquarium technique" as a precision detonation pressure measurement gage. In *Proceedings of the Fifth Symposium (International) on Detonation*; U.S. Naval Ordnance Laboratory and the Office of Naval Research: Pasadena, CA, 1970.

9. Densmore, J.; Biss, M.; McNesby, K.; Homan, B. High-speed digital color imaging pyrometry. *Applied Optics* **2011**, *50* (17), 2659–2665.

10. Deal, W. Low pressure points on the isentropes of several high explosives. In *Proceedings of the Third Symposium (International) on Detonation*; Vol. 386; U.S. Naval Ordnance Laboratory and the Office of Naval Research: Princeton, NJ, 1960.

11. Gruschka, H. D.; Wecken, F. *Gasdynamic Theory of a Detonation*; Gordon and Breach, Science Publishers, Inc.: New York, NY, 1971.

12. Eyring, H.; Powell, R.; Duffy, G.; Parlin, R. The Stability of Detonation. *Chemical Reviews* **1949**, *45* (1), 69–181.

13. Parlin, R. B.; Eyring, H. Interactions of detonation waves with material boundaries. In *Proceedings of the First Symposia on Detonation*; U.S. Naval Ordnance Laboratory and the Office of Naval Research: Washington, D.C., 1951.

14. Taylor, G. The dynamics of the combustion products behind plane and spherical detonation fronts in explosives. *Proceedings of the Royal Society of London.Series A, Mathematical and Physical Sciences* **1950**, *200* (1061), 235–247.

15. Sano, Y. Shock jump equations for unsteady wave fronts. *Journal of Applied Physics* **1997**, *82* (11), 5382–5390.

16. Boegel, A.; Lee, E.; May, C.; Reynolds, J.; Roos, E.; Vitello, P. *"Detonation" in LLNL Explosives Reference Guide*; LLNL-WEB-511311; Lawrence Livermore National Laboratory: Livermore, CA, October 2011.

17. Keshavarz, M.; Pouretedal, H. An empirical method for predicting detonation pressure of CHNOFCl explosives. *Thermochimica Acta* **2004**, *414* (2), 203–208.

18. Moffat, R. J. Describing the uncertainties in experimental results. *Experimental Thermal and Fluid Science* **1988**, *1* (1), 3–17.

19. Allan, J.; Lambourn, B. An equation of state of detonation products at pressures below 30 kilobars. In *Proceedings of the Fourth Symposium (International) on Detonation*; U.S. Naval Ordnance Laboratory and the Office of Naval Research: White Oak, MD, 1965.

20. Roslund, L.; Coleburn, N. L. Hydrodynamic behaviour and equation-of-state of detonation products below the Chapman-Jouguet state. In *Proceedings of the Fifth Symposium (International) on Detonation*; U.S. Naval Ordnance Laboratory and the Office of Naval Research: Pasadena, CA, 1970.

List of Symbols, Abbreviations, and Acronyms

C_0	air bulk sound speed
D	detonation wave velocity
EBW	exploding bridgewire
e	specific internal energy
HBX-1	pourable mixture of RDX, TNT, and aluminum
HMX	cyclotetramethylene tetranitramine
I	explosive impulse
m	explosive charge mass
P	shock wave pressure
P_{CJ}	detonation wave pressure
PETN	pentaerythritol tetranitrate
P_0	atmospheric pressure
RDX	cyclotrimethylene trinitramine
s	air $U - u$ Hugoniot slope
$subscript_0$	properties in front of shock wave
$subscript_1$	properties behind shock wave
T	temperature
T_0	atmospheric temperature
TNT	trinitrotoluene
U	shock wave velocity
u	particle velocity
u_{CJ}	reaction products particle velocity
v	specific volume
ρ_{air}	ambient air density
ρ_{CJ}	reaction products density
ρ_e	energetic material pressing density
W_S	streak camera write speed
Z	shock impedance
Z_{air}	air shock impedance
Z_e	energetic material shock impedance

NO. OF
COPIES   ORGANIZATION

  1   DEFENSE TECHNICAL
 (PDF   INFORMATION CTR
 ONLY)   DTIC OCA
          8725 JOHN J KINGMAN RD
          STE 0944
          FORT BELVOIR VA 22060-6218

  1   DIRECTOR
          US ARMY RESEARCH LAB
          IMNE ALC HRR
          2800 POWDER MILL RD
          ADELPHI MD 20783-1197

  1   DIRECTOR
          US ARMY RESEARCH LAB
          RDRL CIO LL
          2800 POWDER MILL RD
          ADELPHI MD 20783-1197

  1   DIRECTOR
          US ARMY RESEARCH LAB
          RDRL CIO LT
          2800 POWDER MILL RD
          ADELPHI MD 20783-1197

  1   DIRECTOR
          US ARMY RESERACH LAB
          RDRL D
          2800 POWDER MILL RD
          ADELPHI MD 20783-1197

23

2   NAVAL SURF WARFARE CNTR
        N COOK
        L STEELMAN
        6210 TISDALE RD STE 223
        DAHLGREN VA 22448

1   NAVAL SURF WARFARE CNTR
        H HAYDEN
        4081 N JACKSON RD STE 19
        INDIAN HEAD MD 20640

1   NAVAL SURF WARFARE CNTR
        M SHERLOCK
        4103 FOWLER RD SUITE 107
        INDIAN HEAD MD 20640

1   NAVAL SURF WARFARE CNTR
        L NOCK
        4103 FOWLER RD SUITE 119
        INDIAN HEAD MD 20640

2   DTRA
        S PEIRIS
        B WILSON
        8725 JOHN J KINGMAN RD MS 6201
        FORT BELVOIR VA 22060

1   LOS ALAMOS NATL LAB
        D CHAVEZ
        DYN ENERG MATS DIV
        LOS ALAMOS NM 87545

1   LOS ALAMOS NATL LAB
        L PERRY
        PO BOX 1663 MAIL STOP C290
        LOS ALAMOS NM 87545

1   AIR FORCE RSRCH LAB
        RWME
        T KRAWIETZ
        2306 PERIMETER ROAD
        EGLIN AFB FL 32542

ABERDEEN PROVING GROUND

51   US ARMY RESEARCH LAB
DIR USARL
RDRL WML
  M ZOLTOSKI
  J NEWILL
RDRL WML A
  W OBERLE
  F DE LUCIA
  C MUNSON
RDRL WML B
  N TRIVEDI
  J MORRIS
  B RICE
  E BYRD
  R PESCE-RODRIGUEZ
  J GOTTFRIED
  J CIEZAK-JENKINS
  W MATTSON
  R SAUSA
  I BATYREV
  S BUNTE
RDRL WML C
  S AUBERT
  K MCNESBY
  B ROOS
  G SUTHERLAND
  K SPANGLER
  M SHERRILL
  E BUKOWSKI
  T PIEHLER
  V BOYLE
  M BISS (10 CPS)
RDRL WML D
  R BEYER
  B HOMAN
  M NUSCA
  J RITTER
RDRL WML E
  P WEINACHT
RDRL WML F
  D LYON
RDRL WML G
  W DRYSDALE
RDRL WML H
  T BROWN
  M FERMEN-COKER
RDRL WMP A
  B RINGERS
RDRL WMP G

  R EHLERS
  S KUKUCK
RDRL WM
  P BAKER
  B FORCH
  P PLOSTINS
RDRL WMM
  J ZABINSKI

INTENTIONALLY LEFT BLANK.